

## University of Wollongong Research Online

---

Australian Institute for Innovative Materials - Papers

Australian Institute for Innovative Materials

---

2019

# Efficient photocatalytic hydrogen peroxide production over TiO<sub>2</sub> passivated by SnO<sub>2</sub>

Guifu Zuo

*North China University of Science & Technology*

Bingdong Li

*North China University of Science & Technology*

Zhaoliang Guo

*North China University of Science & Technology*

Liang Wang

*University of Wollongong, lw481@uowmail.edu.au*

Fan Yang

*Tianjin University*

*See next page for additional authors*

---

### Publication Details

Zuo, G., Li, B., Guo, Z., Wang, L., Yang, F., Hou, W., Zhang, S., Zong, P., Liu, S., Meng, X., Du, Y., Wang, T. & Roy, V. A. L. (2019). Efficient photocatalytic hydrogen peroxide production over TiO<sub>2</sub> passivated by SnO<sub>2</sub>. *Catalysts*, 9 (7), 623-1-623-9.

Research Online is the open access institutional repository for the University of Wollongong. For further information contact the UOW Library: [research-pubs@uow.edu.au](mailto:research-pubs@uow.edu.au)

---

# Efficient photocatalytic hydrogen peroxide production over TiO<sub>2</sub> passivated by SnO<sub>2</sub>

## Abstract

Photocatalysis provides an attractive strategy for synthesizing H<sub>2</sub>O<sub>2</sub> at ambient condition. However, the photocatalytic synthesis of H<sub>2</sub>O<sub>2</sub> is still limited due to the inefficiency of photocatalysts and decomposition of H<sub>2</sub>O<sub>2</sub> during formation. Here, we report SnO<sub>2</sub>-TiO<sub>2</sub> heterojunction photocatalysts for synthesizing H<sub>2</sub>O<sub>2</sub> directly in aqueous solution. The SnO<sub>2</sub> passivation suppresses the complexation and decomposition of H<sub>2</sub>O<sub>2</sub> on TiO<sub>2</sub>. In addition, loading of Au cocatalyst on SnO<sub>2</sub>-TiO<sub>2</sub> heterojunction further improves the production of H<sub>2</sub>O<sub>2</sub>. The in situ electron spin resonance study revealed that the formation of H<sub>2</sub>O<sub>2</sub> is a stepwise single electron oxygen reduction reaction (ORR) for Au and SnO<sub>2</sub> modified TiO<sub>2</sub> photocatalysts. We demonstrate that it is feasible to enhance H<sub>2</sub>O<sub>2</sub> formation and suppress H<sub>2</sub>O<sub>2</sub> decomposition by surface passivation of the H<sub>2</sub>O<sub>2</sub>-decomposition-sensitive photocatalysts.

## Disciplines

Engineering | Physical Sciences and Mathematics

## Publication Details

Zuo, G., Li, B., Guo, Z., Wang, L., Yang, F., Hou, W., Zhang, S., Zong, P., Liu, S., Meng, X., Du, Y., Wang, T. & Roy, V. A. L. (2019). Efficient photocatalytic hydrogen peroxide production over TiO<sub>2</sub> passivated by SnO<sub>2</sub>. *Catalysts*, 9 (7), 623-1-623-9.

## Authors

Guifu Zuo, Bingdong Li, Zhaoliang Guo, Liang Wang, Fan Yang, Weishu Hou, Songtao Zhang, Peixiao Zong, Shanshan Liu, Xianguang Meng, Yi Du, Tao Wang, and Vellaisamy A. L Roy

Article

# Efficient Photocatalytic Hydrogen Peroxide Production over TiO<sub>2</sub> Passivated by SnO<sub>2</sub>

Guifu Zuo <sup>1</sup>, Bingdong Li <sup>1</sup>, Zhaoliang Guo <sup>1</sup>, Liang Wang <sup>2</sup>, Fan Yang <sup>3</sup>, Weishu Hou <sup>3</sup>, Songtao Zhang <sup>4</sup>, Peixiao Zong <sup>1</sup>, Shanshan Liu <sup>1</sup>, Xianguang Meng <sup>1,5,\*</sup>, Yi Du <sup>2</sup>, Tao Wang <sup>6,\*</sup> and Vellaisamy A. L. Roy <sup>5,7,\*</sup>

<sup>1</sup> Hebei Provincial Key Laboratory of Inorganic Nonmetallic Materials, College of Materials Science and Engineering, North China University of Science and Technology, Tangshan 063210, China

<sup>2</sup> Institute for Superconducting and Electronic Materials, Australian Institute for Innovative Materials, University of Wollongong, Wollongong, New South Wales 2500, Australia

<sup>3</sup> TU-NIMS International Collaboration Laboratory, School of Materials Science and Engineering, Tianjin University, 92 Weijin Road, Tianjin 300072, China

<sup>4</sup> Testing Center, Yangzhou University, Yangzhou 225009, China

<sup>5</sup> Department of Materials Science and Engineering, City University of Hong Kong, Tat Chee Avenue, Kowloon, Hong Kong, China

<sup>6</sup> College of Materials Science and Technology, Jiangsu Key Laboratory of Materials and Technology for Energy Conversion, Nanjing University of Aeronautics and Astronautics, Nanjing 210016, China

<sup>7</sup> State Key Laboratory for THz and Millimeter Waves, City University of Hong Kong, Tat Chee Avenue, Kowloon, Hong Kong, China

\* Correspondence: mengxg\_materchem@163.com (X.M.); wangtao0729@nuaa.edu.cn (T.W.); val.roy@cityu.edu.hk (V.A.L.R.)

Received: 24 June 2019; Accepted: 15 July 2019; Published: 21 July 2019



**Abstract:** Photocatalysis provides an attractive strategy for synthesizing H<sub>2</sub>O<sub>2</sub> at ambient condition. However, the photocatalytic synthesis of H<sub>2</sub>O<sub>2</sub> is still limited due to the inefficiency of photocatalysts and decomposition of H<sub>2</sub>O<sub>2</sub> during formation. Here, we report SnO<sub>2</sub>-TiO<sub>2</sub> heterojunction photocatalysts for synthesizing H<sub>2</sub>O<sub>2</sub> directly in aqueous solution. The SnO<sub>2</sub> passivation suppresses the complexation and decomposition of H<sub>2</sub>O<sub>2</sub> on TiO<sub>2</sub>. In addition, loading of Au cocatalyst on SnO<sub>2</sub>-TiO<sub>2</sub> heterojunction further improves the production of H<sub>2</sub>O<sub>2</sub>. The in situ electron spin resonance study revealed that the formation of H<sub>2</sub>O<sub>2</sub> is a stepwise single electron oxygen reduction reaction (ORR) for Au and SnO<sub>2</sub> modified TiO<sub>2</sub> photocatalysts. We demonstrate that it is feasible to enhance H<sub>2</sub>O<sub>2</sub> formation and suppress H<sub>2</sub>O<sub>2</sub> decomposition by surface passivation of the H<sub>2</sub>O<sub>2</sub>-decomposition-sensitive photocatalysts.

**Keywords:** H<sub>2</sub>O<sub>2</sub>; single electron ORR; SnO<sub>2</sub>-TiO<sub>2</sub>; passivation

## 1. Introduction

Hydrogen peroxide (H<sub>2</sub>O<sub>2</sub>) is a clean oxidant [1] that has wide applications in environmental purification and organic synthesis [2]. At present, H<sub>2</sub>O<sub>2</sub> is industrially produced by the multi-step anthraquinone method, which consumes a lot of energy and organic solvent [3]. As an alternative to the anthraquinone method, direct photocatalytic synthesis of H<sub>2</sub>O<sub>2</sub> has attracted widespread attention due to its mild reaction conditions, such as normal temperature and pressure under light irradiation. Many representative UV-light and visible-light active semiconductors (e.g., ZnO [4,5], C<sub>3</sub>N<sub>4</sub> [6–9], BiVO<sub>4</sub> [10], etc.) have been verified as active materials for H<sub>2</sub>O<sub>2</sub> production, particularly when proper cocatalysts are loaded on these semiconductors. An important feature of photocatalytic H<sub>2</sub>O<sub>2</sub> formation is that it is accompanied by a decomposition process. TiO<sub>2</sub> is a widely used photocatalyst for synthesizing H<sub>2</sub>O<sub>2</sub>

directly from O<sub>2</sub> reduction in liquid phase under the irradiation of ultraviolet (UV) light [3,11–17], without using hydrogen. However, photocatalytic H<sub>2</sub>O<sub>2</sub> synthesis with TiO<sub>2</sub> has a low formation reaction rate due to the catalytic decomposition [17,18]. Some studies have revealed the decomposition mechanism of H<sub>2</sub>O<sub>2</sub> in aqueous TiO<sub>2</sub> suspension under UV irradiation [18–20]. Zhao et al. [18] reported that adsorption of H<sub>2</sub>O<sub>2</sub> on TiO<sub>2</sub> will readily form surface peroxide complexes, which can be easily photodegraded with a zero-order kinetic process over TiO<sub>2</sub> even with the irradiation of visible light, thus leading to the decrease of H<sub>2</sub>O<sub>2</sub> production. Therefore, in order to produce concentrated H<sub>2</sub>O<sub>2</sub>, on one hand, the formation rate of H<sub>2</sub>O<sub>2</sub> should be increased, and on the other hand, the decomposition of H<sub>2</sub>O<sub>2</sub> should be controlled.

Au is an active cocatalyst and has shown great potential in improving the performance of photocatalytic H<sub>2</sub>O<sub>2</sub> production [15,16]. Tada et al. [15] reported enhancement of the photocatalytic activity of TiO<sub>2</sub> in producing H<sub>2</sub>O<sub>2</sub> by Au cocatalyst loading. They also found that the formation of H<sub>2</sub>O<sub>2</sub> was generally accompanied by decomposition. The concentration of H<sub>2</sub>O<sub>2</sub> produced from the photocatalytic reduction of O<sub>2</sub> can also be increased by restricting its thermocatalytic decomposition through controlling the temperature and pH of the reaction solution [16]. Indeed, these studies improved H<sub>2</sub>O<sub>2</sub> formation activity by suppressing the decomposition process by controlling the reaction condition. However, there is still no effective means of enhancing the intrinsic activity of photocatalysts for H<sub>2</sub>O<sub>2</sub> production. It is well known that both the structures and band gaps of TiO<sub>2</sub> and SnO<sub>2</sub> are similar. They all consist of MO<sub>6</sub> octahedrons as the structural unit. The conduction band (CB) of SnO<sub>2</sub> (0 V vs. SHE) is more positive than that of the TiO<sub>2</sub> (−0.3 V vs. SHE) and it is possible to improve charge separation in a photocatalytic reaction when heterojunctions are formed by both oxides [21–23]. In this study, we prepared SnO<sub>2</sub>-modified anatase TiO<sub>2</sub> (SnO<sub>2</sub>-TiO<sub>2</sub>) heterojunction using the molten salt method [24]. SnO<sub>2</sub> passivation suppressed H<sub>2</sub>O<sub>2</sub> complexation and decomposition on the surface of TiO<sub>2</sub>. Loading of Au nanococatalysts further remarkably enhanced the H<sub>2</sub>O<sub>2</sub> formation rate.

## 2. Results and Discussion

### 2.1. Characterization of the Photocatalysts

Figure 1a shows the XRD patterns of 0.1% Au loaded SnO<sub>2</sub>-TiO<sub>2</sub> obtained at different sintering temperatures. When the sintering temperature is 300 °C, almost no SnO<sub>2</sub> can be detected. It has been well documented that the melting point of LiCl-KCl eutectic of composition 61:39 is 352 °C [24]. Hence, the Sn precursor is impossible to dissolve by molten salt and SnO<sub>2</sub> cannot be formed on the TiO<sub>2</sub> at this temperature. The presence of SnO<sub>2</sub> can be identified when the sintering temperature reaches 400 °C. At a sintering temperature of 500 °C, the peak of SnO<sub>2</sub> becomes more obvious, implying higher modification of SnO<sub>2</sub>. At the sintering temperature of 600 °C, anatase was partially transformed into a less active rutile phase [25]. The diffraction peaks of SnO<sub>2</sub> can be clearly identified with the increase in the Sn/Ti ratio (Figure 1b). The presence of SnO<sub>2</sub> and Au are certified by the EDX (Figure S1). STEM mapping images (Figure 1c–f) display that SnO<sub>2</sub> and Au are finely dispersed on the surface of TiO<sub>2</sub>. Formation of such a SnO<sub>2</sub>-TiO<sub>2</sub> heterojunction structure will improve the charge separation and photocatalytic activity [21–23].

As shown in Figure 1g, there are two prominent absorption bands in the UV-Vis spectra of Au/SnO<sub>2</sub>-TiO<sub>2</sub>. Besides the characteristic absorption bands of TiO<sub>2</sub> at 370 nm, the broad absorption bands in the visible region between 500 nm and 650 nm is due to the excitation of gold surface plasmon. In addition, the nanometal cocatalyst exhibit lattice fringes of 0.235 nm, which matches the interplanar spacing of Au (1 1 1) plane (Figure S2) [26]. The actual content of Au in 0.1% Au/SnO<sub>2</sub>-TiO<sub>2</sub> was 0.106% by inductively coupled plasma mass spectrometry (ICP-MS).

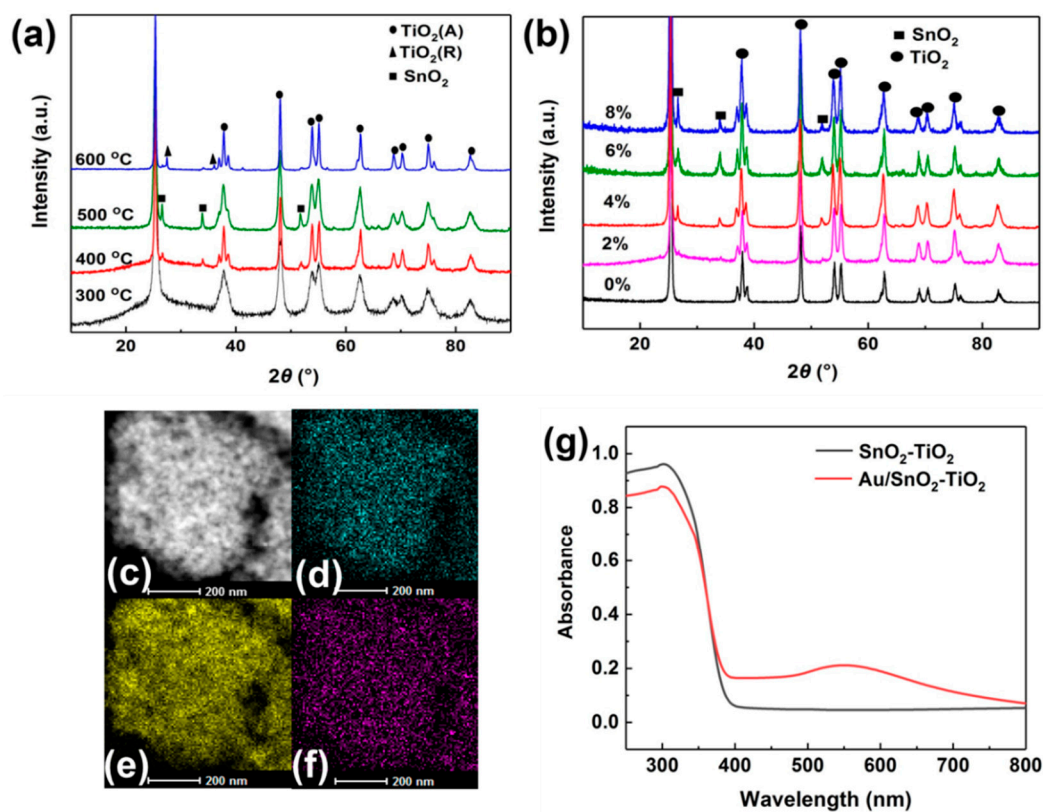


**Figure 1.** (a) XRD patterns of 0.1% Au loaded SnO<sub>2</sub>-TiO<sub>2</sub> (4% SnO<sub>2</sub> modified anatase TiO<sub>2</sub>) obtained at different sintering temperatures. (b) XRD patterns of 0.1% Au loaded SnO<sub>2</sub>-TiO<sub>2</sub> with different Sn/Ti ratios. (c) HAADF-STEM images of 0.1% Au loaded SnO<sub>2</sub>-TiO<sub>2</sub> (Sn/Ti is 4%). (d–f) Mapping images of (d) Sn, (e) Ti and (f) Au elements. (g) UV-vis spectra of SnO<sub>2</sub>-TiO<sub>2</sub> with and without 0.1% Au.

## 2.2. Catalytic Activity of the Photocatalysts

The photocatalytic activity of H<sub>2</sub>O<sub>2</sub> synthesis on Au/SnO<sub>2</sub>-TiO<sub>2</sub> hybrids was tested under UV light and the concentration of H<sub>2</sub>O<sub>2</sub> was quantified by spectrophotometry with copper ions and 2,9-dimethyl-1,10-phenanthroline (DMP) [27]. The standard curve indicates that the absorbance and concentration of H<sub>2</sub>O<sub>2</sub> exhibits a good linear relationship with R square of 0.9996 (Figure S3). Figure 2a shows time courses for the H<sub>2</sub>O<sub>2</sub> generation of photocatalysts obtained at different sintering temperatures. Noticeably, 0.1% Au loaded SnO<sub>2</sub>-TiO<sub>2</sub> obtained at 500 °C exhibits the highest photocatalytic activity compared to that obtained at the other sintering temperatures. In combination with XRD data, when the sintering temperature is 300 °C, the content of SnO<sub>2</sub> in the samples is minimal, and the activity is not obviously improved. The photocatalytic activity of the samples obtained at 600 °C is the lowest, possibly because of the formation of a less active rutile phase.

Compared with pristine Au/TiO<sub>2</sub>, Au/SnO<sub>2</sub>-TiO<sub>2</sub> hybrids exhibited enhanced photocatalytic activity (Figure 2b). The highest photocatalytic activity was obtained over the sample with a Sn/Ti ratio of 4%, which also showed stable H<sub>2</sub>O<sub>2</sub> production rate. The improved activity is mainly due to the suppression of H<sub>2</sub>O<sub>2</sub> decomposition by SnO<sub>2</sub> passivation as discussed below. The excessive SnO<sub>2</sub> modification will possibly shield the photo absorption of TiO<sub>2</sub>, and thus reduce the photocatalytic activity. It should be noted that we also did a control experiment, which is shown in Figure S4. It was found that there is a synergistic effect between Au and SnO<sub>2</sub> in H<sub>2</sub>O<sub>2</sub> synthesis over TiO<sub>2</sub>.

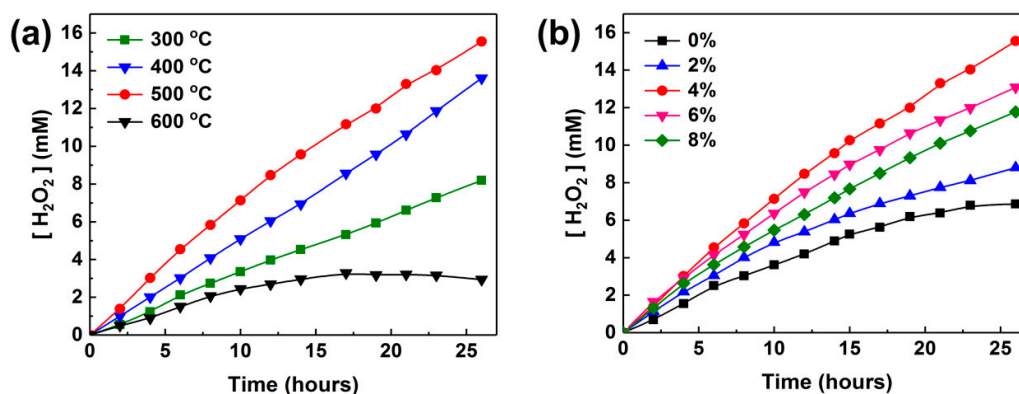


**Figure 2.** (a) Plots of [H<sub>2</sub>O<sub>2</sub>] under UV-irradiation in the presence of 0.1% Au loaded SnO<sub>2</sub>-TiO<sub>2</sub> (4% SnO<sub>2</sub> modified anatase TiO<sub>2</sub>) obtained at different sintering temperatures. (b) Plots of [H<sub>2</sub>O<sub>2</sub>] under UV-irradiation in the presence of 0.1% Au loaded SnO<sub>2</sub>-TiO<sub>2</sub> with different Sn/Ti ratios.

### 2.3. ESR Analysis

In general, H<sub>2</sub>O<sub>2</sub> from 2e<sup>-</sup> ORR by CB electrons can be produced through stepwise coupled electron and proton transfers (Equations (1)–(3)) [28,29]. In order to further study the formation mechanism of H<sub>2</sub>O<sub>2</sub>, in situ ESR measurements were carried out using DMPO as the trapper of radical species. The radical signals of DMPO-•OOH consisting of six characteristic peaks were detected for all of Au and/or SnO<sub>2</sub> modified TiO<sub>2</sub>, while there is no obvious signals for pure TiO<sub>2</sub> (Figure 3a,b), showing that H<sub>2</sub>O<sub>2</sub> formation over Au loaded and/or SnO<sub>2</sub> modified TiO<sub>2</sub> photocatalysts is indeed a stepwise single electron reduction process, and both Au and SnO<sub>2</sub> could promote the formation of HO<sub>2</sub>• via Equation (2).

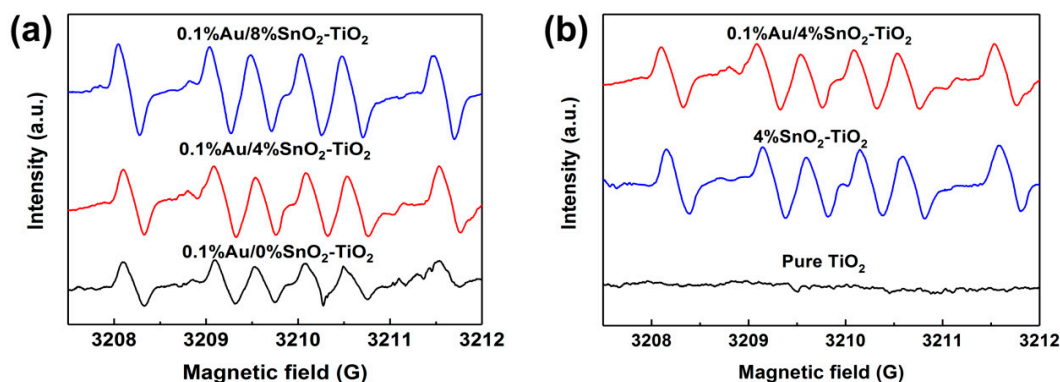


**Figure 3.** (a) In situ ESR spectra of the 0.1% Au/SnO<sub>2</sub>-TiO<sub>2</sub> samples with different Sn/Ti ratios under UV light irradiation. (b) In situ ESR spectra of the samples (4% SnO<sub>2</sub> modified anatase TiO<sub>2</sub>) with and without Au cocatalyst under UV light irradiation.

### 2.4. The Photodecomposition of H<sub>2</sub>O<sub>2</sub>

Figure 4 shows the decomposition of H<sub>2</sub>O<sub>2</sub> under different conditions. Pure H<sub>2</sub>O<sub>2</sub> remains stable under dark conditions in the presence of 0.1% Au/SnO<sub>2</sub>-TiO<sub>2</sub> (4% Sn/Ti ratio) (Figure 4a). Under UV irradiation without catalyst, the decomposition of H<sub>2</sub>O<sub>2</sub> has a linear relationship with time. In the presence of TiO<sub>2</sub>, 0.1% Au/TiO<sub>2</sub> or 0.1% Au/SnO<sub>2</sub>-TiO<sub>2</sub>, the H<sub>2</sub>O<sub>2</sub> decomposition was accelerated by

UV light, but the decomposition rate of  $\text{H}_2\text{O}_2$  over 0.1%  $\text{Au}/\text{SnO}_2\text{-TiO}_2$  is lower than  $\text{TiO}_2$  and 0.1%  $\text{Au}/\text{TiO}_2$ . The relationship between hydrogen peroxide decomposition and time is nonlinear under UV irradiation, and the decomposition of  $\text{H}_2\text{O}_2$  is similar to a one-order kinetics [30]. In order to investigate the decomposition solely induced by peroxide complexes, we tested the decomposition of  $\text{H}_2\text{O}_2$  in an aqueous photocatalyst suspension with similar initial  $\text{H}_2\text{O}_2$  concentrations under visible light irradiation (Figure 4b).  $\text{H}_2\text{O}_2$  barely decomposed under dark conditions in an aqueous  $\text{SnO}_2\text{-TiO}_2$  suspension or under visible light irradiation without any photocatalysts. In the presence of photocatalysts, the  $\text{H}_2\text{O}_2$  decomposition was accelerated, but again,  $\text{SnO}_2$  passivated  $\text{TiO}_2$  had the lowest decomposition activity. All the decomposition processes under visible light irradiation can be roughly fitted with a near zero-order equation (linear relationship) [18]. It can be inferred that there is a synergistic effect between the photocatalysts and light irradiation in catalyzing  $\text{H}_2\text{O}_2$  decomposition. However,  $\text{SnO}_2$  passivated  $\text{TiO}_2$  consistently showed suppressed decomposition activity in any condition (UV and visible light). It is important for  $\text{SnO}_2\text{-TiO}_2$  heterojunction photocatalyst to maintain high and stable  $\text{H}_2\text{O}_2$  production rate during the photocatalytic reaction. The generation and decomposition mechanism of  $\text{H}_2\text{O}_2$  is shown in Figure 5. The electrons excited by UV light are transferred to the Au and  $\text{SnO}_2$  to promote reduction of  $\text{O}_2$  for  $\text{H}_2\text{O}_2$  formation. Compared with easy  $\text{H}_2\text{O}_2$  decomposition on pure  $\text{TiO}_2$  via forming peroxide complexes,  $\text{SnO}_2$  passivated  $\text{TiO}_2$  suppressed  $\text{H}_2\text{O}_2$  decomposition. Hence, this study provides a useful method for promoting  $\text{H}_2\text{O}_2$  production over  $\text{TiO}_2$  photocatalysts.

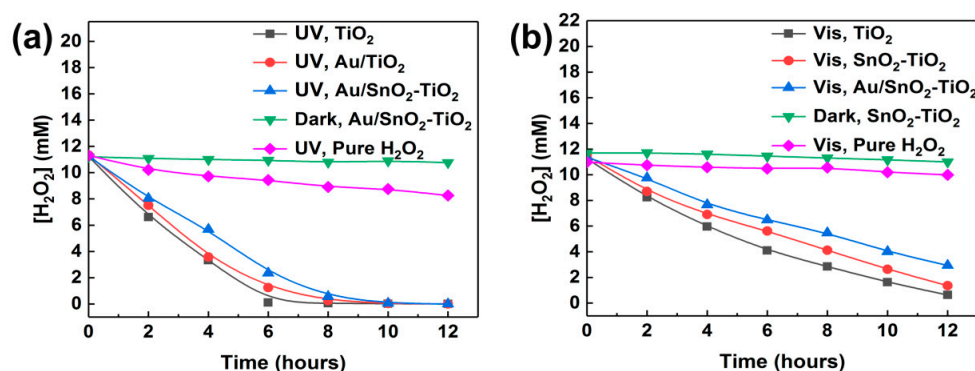


Figure 4.  $\text{H}_2\text{O}_2$  photodecomposition under UV light (a) and visible light (b) conditions.

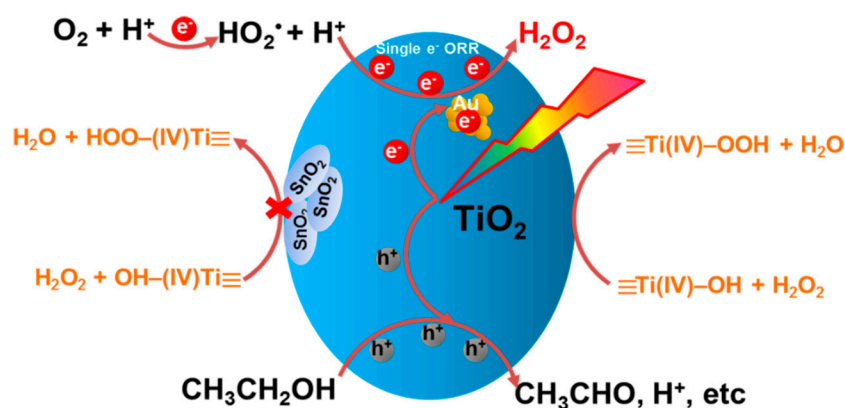


Figure 5. Schematic illustration of  $\text{H}_2\text{O}_2$  synthesis and decomposition over  $\text{Au}/\text{SnO}_2\text{-TiO}_2$ .

### 3. Materials and Methods

#### 3.1. Materials Preparation

To produce a SnO<sub>2</sub>-TiO<sub>2</sub> heterojunction structure, anatase TiO<sub>2</sub> powder (with a grain size of 5 nm and a specific surface area of 280 m<sup>2</sup>/g, Yifu Industrial Co., Ltd, Shanghai, China) was used as a photocatalyst. SnCl<sub>4</sub>•4H<sub>2</sub>O (Sinopharm Chemical Reagent Co., Ltd, Shanghai, China) was used to modify TiO<sub>2</sub> by a molten salt method. In general, 3.4 g anatase TiO<sub>2</sub> and 0.6 g SnCl<sub>4</sub>•4H<sub>2</sub>O (4% molar ratio of Sn:Ti) were mixed with 3.77 g LiCl (Yongda Chemical Reagent Co., Ltd, Tianjin, China) and 4.23 g KCl (Yongda Chemical Reagent Co., Ltd, Tianjin, China) in an alumina crucible. The powder mixtures were calcined at 500 °C, then the mixtures were transferred into the deionized water for grinding, centrifuged, washed and dried. The Au with 0.1 wt % was loaded on photocatalysts by the deposition-precipitation method reported previously [31]. The decomposition of H<sub>2</sub>O<sub>2</sub> can be suppressed to a certain extent by sodium fluoride. SnO<sub>2</sub>-TiO<sub>2</sub> can produce valence band electrons and holes by UV irradiation.

#### 3.2. Material Characterization

The powder X-ray diffraction (XRD) data were collected on an X-ray diffractometer (D/Ma-2500, Rigaku, Tokyo, Japan) operating with Cu K $\alpha$  radiation ( $\lambda = 0.15406$  nm). UV-VIS spectra were recorded with a Spectrum Lambda 750 S (Perkin-Elmer, Waltham, MA, USA). High-resolution transmission electron microscopy (TEM) characterization was performed with 8000EX microscope (JEOL, Tokyo, Japan) operating at 200 kV.

#### 3.3. Photocatalytic Reactivity Test

A photocatalytic reaction kettle (200 mL) was used as a photocatalytic reaction device. NaF (0.1 M, Shentai Chemical Reagent Co., Ltd, Tianjin, China) was added as part of reaction medium together with 0.2 g Au/SnO<sub>2</sub>-TiO<sub>2</sub> into the reaction solution of alcohol (4 wt %) and deionized water. The suspension solution was under ultrasonic treatment for 2 to 3 min. Then the mixed solution was poured into the reaction kettle and the oxygen was passed for 30 min. Then, a 300 W Xe arc lamp (PLS-SXE300, Bofeilai Technology Co., Ltd, Beijing, China) was used as a light source and was turned on the solution. The light was emitted by the xenon lamp and reflected by the UV light reflector. Magnetic stirring of the suspension was maintained throughout the reaction. The condensate water continued to pass the reaction kettle. Then, the concentrations of H<sub>2</sub>O<sub>2</sub> generated were determined by using the DMP (2,9-dimethyl-1,10-phenanthroline, Wengjiang Chemical Reagent Co., Ltd, Guangdong, China) method [27].

#### 3.4. Quantification of H<sub>2</sub>O<sub>2</sub> (DMP Method)

One mL of DMP (0.1 g/L), 1 mL of copper (II) sulfate (0.1 M), and 1 mL of phosphate buffer (pH 7.0) solution, and 1 mL of reaction solution were added to a 10 mL volumetric flask and was mixed, and then deionized water was added to the volumetric flask to the tick mark. After mixing, the absorbance of the sample at 454 nm was measured. The blank solution was prepared in the same manner but without H<sub>2</sub>O<sub>2</sub>.

The concentrations of H<sub>2</sub>O<sub>2</sub> were calculated by the following formula:

$$A_{454} = \zeta [H_2O_2] \times 1/10$$

where  $A_{454}$  is the difference of the absorbance between sample and blank solutions at 454 nm,  $\zeta$  is the slope of the calibration curve, and  $[H_2O_2]$  is the H<sub>2</sub>O<sub>2</sub> concentration ( $\mu$ M).



### 3.5. Photocatalytic H<sub>2</sub>O<sub>2</sub> Decomposition

Basically, photocatalytic H<sub>2</sub>O<sub>2</sub> decomposition was carried out in the same reaction medium for photocatalytic H<sub>2</sub>O<sub>2</sub> synthesis. Photocatalyst (0.2 g) was dispersed in water (200 mL) containing NaF (0.1 M), 4% C<sub>2</sub>H<sub>5</sub>OH (99.7%, Yongda Chemical Reagent Co., Ltd, Tianjin, China) and H<sub>2</sub>O<sub>2</sub> (30%, Yongda Chemical Reagent Co., Ltd, Tianjin, China) with a fixed concentration. The suspension was stirred in the dark conditions for 30 min under constant N<sub>2</sub> bubbling to remove the air before light irradiation.

### 3.6. In Situ ESR Test

In situ electron spin resonance (ESR) analysis was performed to confirm the reduction pathway of O<sub>2</sub> over different catalysts, which uses 5,5-dimethyl-1-pyrroline N-oxide (DMPO) as a spin-trapping reagent. ESR signals of radicals trapped by DMPO were detected with a ESP 300E spectrometer (Bruker, Switzerland). Typically, catalyst (1 mg) was added to a mixture containing 1 mL alcohol/water (4 wt %) and 0.125 mmol DMPO. After passing the O<sub>2</sub> for 3 min, the sample was irradiated under UV light for 5 min before testing.

## 4. Conclusions

Au-modified SnO<sub>2</sub>-TiO<sub>2</sub> was successfully prepared for enhanced photocatalytic activity for H<sub>2</sub>O<sub>2</sub> production. The SnO<sub>2</sub>-TiO<sub>2</sub> (4% SnO<sub>2</sub> modified anatase TiO<sub>2</sub>) heterojunction prepared at 500 °C showed the best performance. H<sub>2</sub>O<sub>2</sub> formed through a stepwise single electron reduction process over Au and/or SnO<sub>2</sub> modified TiO<sub>2</sub> via the formation of HO<sub>2</sub>• intermediate. Under the band-gap excitation with UV light, decomposition of H<sub>2</sub>O<sub>2</sub> seems to conform to a one-order kinetics process. SnO<sub>2</sub> passivation suppressed the decomposition of H<sub>2</sub>O<sub>2</sub> over TiO<sub>2</sub> under both UV and visible light. This study provides a useful strategy to improve the performance of TiO<sub>2</sub> by modifying H<sub>2</sub>O<sub>2</sub>-inert oxide to decrease the decomposition of H<sub>2</sub>O<sub>2</sub> during its photocatalytic synthesis.

**Supplementary Materials:** The following are available online at <http://www.mdpi.com/2073-4344/9/7/623/s1>, Figure S1: (TEM images of Au/SnO<sub>2</sub> TiO<sub>2</sub> and (b) EDX result of the square area in (a), Figure S2: (a) TEM images of Au/SnO<sub>2</sub> TiO<sub>2</sub> and (b) the measured interplanar spacing (0.235 nm) of Au (1 1 1) plane, Figure S3: Standard curve: a linear relationship for the optical absorbance at 454 nm as a function of H<sub>2</sub>O<sub>2</sub> concentration, Figure S4: Plots of [H<sub>2</sub>O<sub>2</sub>] under UV-irradiation in the presence of different photocatalysts.

**Author Contributions:** G.Z., B.L. and Z.G. carried out the experimental work and prepared the manuscript. L.W., Y.D., and S.Z. tested the STEM of samples and provided useful suggestions to this work. The corresponding author X.M. directed the experimental work and paper writing. T.W. and V.A.L.R. were involved in the discussion and provided useful suggestions to this work. W.H. and F.Y. provided assistance in the test of in situ ESR and ICP-MS at Tianjin University. P.Z. and S.L. from the North China University of Science and Technology provided assistance with the experimental work.

**Funding:** This work was supported by the National Natural Science Foundation of China (51872091, 51502075, 21703065, and 51602153), “Hundred Talents Program” of Hebei Province (E2018050013), Natural Science Foundation of Hebei Province (B2018209267), Outstanding Youth Funds of North China University of Science and Technology (JP201604 and JQ201706), and the Hong Kong Scholars Program. Guifu Zuo, Bingdong Li, and Zhaoliang Guo contributed equally to this work.

**Conflicts of Interest:** There are no conflict to declare.

## References

1. Sato, K.; Aoki, M.; Noyori, R. A “Green” Route to Adipic Acid: Direct Oxidation of Cyclohexenes with 30 Percent Hydrogen Peroxide. *Science* **1998**, *281*, 1646–1647. [[CrossRef](#)] [[PubMed](#)]
2. Samanta, C. Direct synthesis of hydrogen peroxide from hydrogen and oxygen: An overview of recent developments in the process. *Appl. Catal. A Gen.* **2008**, *350*, 133–149. [[CrossRef](#)]
3. Moon, G.H.; Kim, W.; Bokare, A.D.; Sung, N.E.; Choi, W. Solar production of H<sub>2</sub>O<sub>2</sub> on reduced graphene oxide-TiO<sub>2</sub> hybrid photocatalysts consisting of earth-abundant elements only. *Energy Environ. Sci.* **2014**, *7*, 4023–4028. [[CrossRef](#)]

4. Domènech, X.; Ayllón, J.A.; Peral, J. H<sub>2</sub>O<sub>2</sub> Formation from photocatalytic processes at the ZnO/water interface. *Environ. Sci. Pollut. Res.* **2001**, *8*, 285–287. [[CrossRef](#)]
5. Kormann, C.; Bahnemann, D.W.; Hoffmann, M.R. Environmental photochemistry: Is iron oxide (hematite) an active photocatalyst? A comparative study:  $\alpha$ -Fe<sub>2</sub>O<sub>3</sub>, ZnO, TiO<sub>2</sub>. *J. Photochem. Photobiol. A Chem.* **1989**, *48*, 161–169. [[CrossRef](#)]
6. Shi, L.; Yang, L.; Zhou, W.; Liu, Y.; Yin, L.; Hai, X.; Song, H.; Ye, J. Photoassisted Construction of Holey Defective g-C<sub>3</sub>N<sub>4</sub> Photocatalysts for Efficient Visible-Light-Driven H<sub>2</sub>O<sub>2</sub> Production. *Small* **2018**, *14*, 1703142. [[CrossRef](#)] [[PubMed](#)]
7. Shiraishi, Y.; Kanazawa, S.; Sugano, Y.; Tsukamoto, D.; Sakamoto, H.; Ichikawa, S.; Hirai, T. Highly Selective Production of Hydrogen Peroxide on Graphitic Carbon Nitride (g-C<sub>3</sub>N<sub>4</sub>) Photocatalyst Activated by Visible Light. *ACS Catal* **2016**, *4*, 774–780. [[CrossRef](#)]
8. Zhu, Z.; Pan, H.; Murugananthan, M.; Gong, J.; Zhang, Y. Visible light-driven photocatalytically active g-C<sub>3</sub>N<sub>4</sub> material for enhanced generation of H<sub>2</sub>O<sub>2</sub>. *Appl. Catal. B Environ.* **2018**, *232*, 19–25. [[CrossRef](#)]
9. Zuo, G.; Liu, S.; Wang, L.; Song, H.; Zong, P.; Hou, W.; Li, B.; Guo, Z.; Meng, X.; Du, Y.; et al. Finely dispersed Au nanoparticles on graphitic carbon nitride as highly active photocatalyst for hydrogen peroxide production. *Catal. Commun.* **2019**, *123*, 69–72. [[CrossRef](#)]
10. Hirakawa, H.; Shiota, S.; Shiraishi, Y.; Sakamoto, H.; Hirai, T. Au Nanoparticles Supported on BiVO<sub>4</sub>: Effective Inorganic Photocatalysts for H<sub>2</sub>O<sub>2</sub> Production from Water and O<sub>2</sub> under Visible Light. *ACS Catal* **2016**, *6*, 4976–4982. [[CrossRef](#)]
11. Cai, R.; Kubota, Y.; Fujishima, A. Effect of copper ions on the formation of hydrogen peroxide from photocatalytic titanium dioxide particles. *J. Catal.* **2003**, *219*, 214–218. [[CrossRef](#)]
12. Daimon, T.; Hirakawa, T.; Kitazawa, M.; Suetake, J.; Nosaka, Y. Formation of singlet molecular oxygen associated with the formation of superoxide radicals in aqueous suspensions of TiO<sub>2</sub> photocatalysts. *Appl. Catal. A Gen.* **2008**, *340*, 169–175. [[CrossRef](#)]
13. Goto, H.; Hanada, Y.; Ohno, T.; Matsumura, M. Quantitative analysis of superoxide ion and hydrogen peroxide produced from molecular oxygen on photoirradiated TiO<sub>2</sub> particles. *J. Catal.* **2004**, *225*, 223–229. [[CrossRef](#)]
14. Zheng, L.; Su, H.; Zhang, J.; Walekar, L.S.; Vafaei, M.H.; Zhou, B.; Long, M.; Hu, Y.H. Highly selective photocatalytic production of H<sub>2</sub>O<sub>2</sub> on sulfur and nitrogen co-doped graphene quantum dots tuned TiO<sub>2</sub>. *Appl. Catal. B* **2018**, *475*–484. [[CrossRef](#)]
15. Teranishi, M.; Naya, S.I.; Tada, H. In situ liquid phase synthesis of hydrogen peroxide from molecular oxygen using gold nanoparticle-loaded titanium(IV) dioxide photocatalyst. *J. Am. Chem. Soc.* **2010**, *132*, 7850–7851. [[CrossRef](#)]
16. Teranishi, M.; Naya, S.I.; Tada, H. Temperature-And pH-Dependences of In Situ Liquid-Phase Hydrogen Peroxide Formation from Molecular Oxygen by Gold Nanoparticle-Loaded Titanium (IV) Oxide Photocatalyst. *J. Phys. Chem. C* **2016**, *120*, 1083–1088. [[CrossRef](#)]
17. Tsukamoto, D.; Shiro, A.; Shiraishi, Y.; Sugano, Y.; Ichikawa, S.; Tanaka, S.; Hirai, T. Photocatalytic H<sub>2</sub>O<sub>2</sub> Production from Ethanol/O<sub>2</sub> System Using TiO<sub>2</sub> Loaded with Au-Ag Bimetallic Alloy Nanoparticles. *ACS Catal.* **2012**, *2*, 599–603. [[CrossRef](#)]
18. Li, X.; Chen, C.; Zhao, J. Mechanism of Photodecomposition of H<sub>2</sub>O<sub>2</sub> on TiO<sub>2</sub> Surfaces under Visible Light Irradiation. *Langmuir* **2001**, *17*, 4118–4122. [[CrossRef](#)]
19. Harbour, J.R.; Tromp, J.; Hair, M.L. Photogeneration of hydrogen peroxide in aqueous TiO<sub>2</sub> dispersions. *Can. J. Chem.* **1985**, *63*, 204–208. [[CrossRef](#)]
20. Kormann, C.; Bahnemann, D.W.; Hoffmann, M.R. Photocatalytic production of hydrogen peroxides and organic peroxides in aqueous suspensions of titanium dioxide, zinc oxide, and desert sand. *Environ. Sci. Technol.* **1988**, *22*, 798–806. [[CrossRef](#)]
21. Mendonça, V.R.D.; Avansi, W., Jr.; Arenal, R.; Ribeiro, C. A building blocks strategy for preparing photocatalytically active anatase TiO<sub>2</sub>/rutile SnO<sub>2</sub> heterostructures by hydrothermal annealing. *J. Colloid. Interface Sci.* **2018**, *505*, 454–459. [[CrossRef](#)]
22. Ohsaki, H.; Kanai, N.; Fukunaga, Y.; Suzuki, M.; Watanabe, T.; Hashimoto, K. Photocatalytic properties of SnO<sub>2</sub>/TiO<sub>2</sub> multilayers. *Thin Solid Film.* **2006**, *502*, 138–142. [[CrossRef](#)]

23. Yuan, J.; Zhang, X.; Li, H.; Kai, W.; Gao, S.; Zhen, Y.; Yu, H.; Zhu, X.; Xiong, Z.; Xie, Y. TiO<sub>2</sub>/SnO<sub>2</sub> double-shelled hollow spheres-highly efficient photocatalyst for the degradation of rhodamine B. *Catal. Commun.* **2015**, *60*, 129–133. [[CrossRef](#)]
24. Naidu, H.P.; Virkar, A.V. Low-Temperature TiO<sub>2</sub>-SnO<sub>2</sub> Phase Diagram Using the Molten-Salt Method. *J. Am. Ceram. Soc.* **2010**, *81*, 2176–2180. [[CrossRef](#)]
25. Jung, H.S.; Kim, H. Origin of low photocatalytic activity of rutile TiO<sub>2</sub>. *Electron. Mater. Lett.* **2009**, *5*, 73–76. [[CrossRef](#)]
26. Alshammari, A.; Bagabas, A.; Assulami, M. Photodegradation of rhodamine B over semiconductor supported gold nanoparticles: The effect of semiconductor support identity. *Arab. J. Chem.* **2015**, *29*, 1–20. [[CrossRef](#)]
27. Kosaka, K.; Yamada, H.; Matsui, S.; Echigo, S.; Shishida, K. Comparison among the Methods for Hydrogen Peroxide Measurements To Evaluate Advanced Oxidation Processes: Application of a Spectrophotometric Method Using Copper(II) Ion and 2, 9-Dimethyl-1, 10-phenanthroline. *Environ. Sci. Technol.* **1998**, *32*, 3821–3824. [[CrossRef](#)]
28. Samira, S.; Arnau, V.C.; Mohammadreza, K.; Davide, D.; Paolo, M.; Björn, W.; María, E.E.; Paoli, E.A.; Rasmus, F.; Hansen, T.W. Enabling direct H<sub>2</sub>O<sub>2</sub> production through rational electrocatalyst design. *Nat. Mater.* **2013**, *12*, 1137–1143.
29. Viswanathan, V.; Hansen, H.A.; Rossmeisl, J.; Nørskov, J.K. Unifying the 2e(-) and 4e(-) Reduction of Oxygen on Metal Surfaces. *J. Phys. Chem. Lett.* **2012**, *3*, 2948–2951. [[CrossRef](#)]
30. Maurino, V.; Minero, C.; Mariella, G.; Pelizzetti, E. Sustained production of H<sub>2</sub>O<sub>2</sub> on irradiated TiO<sub>2</sub>-fluoride systems. *Chem. Commun.* **2005**, *36*, 2627–2629. [[CrossRef](#)]
31. Liu, L.; Li, P.; Adisak, B.; Ouyang, S.; Umezawa, N.; Ye, J.; Kodiyath, R.; Tanabe, T.; Ramesh, G.V.; Ueda, S. Gold photosensitized SrTiO<sub>3</sub> for visible-light water oxidation induced by Au interband transitions. *J. Mater. Chem. A* **2014**, *2*, 9875–9882. [[CrossRef](#)]



© 2019 by the authors. Licensee MDPI, Basel, Switzerland. This article is an open access article distributed under the terms and conditions of the Creative Commons Attribution (CC BY) license (<http://creativecommons.org/licenses/by/4.0/>).